

## 5G cascaded channel estimation using convolutional neural networks

Fábio D.L. Coutinho <sup>a,\*</sup>, Hugerles S. Silva <sup>a,b</sup>, Petia Georgieva <sup>c</sup>, Arnaldo S.R. Oliveira <sup>a</sup>



<sup>a</sup> Instituto de Telecomunicações e Departamento de Electrónica, Telecomunicações e Informática, Universidade de Aveiro, Campus Universitário de Santiago, 3810-193 Aveiro, Portugal

<sup>b</sup> Department of Electrical Engineering, University of Brasília (UnB), Brasília 70910-900, Brazil

<sup>c</sup> Instituto de Engenharia Electrónica e Telemática de Aveiro e Departamento de Electrónica, Telecomunicações e Informática, Universidade de Aveiro, Campus Universitário de Santiago, 3810-193 Aveiro, Portugal

### ARTICLE INFO

#### Article history:

Available online 19 February 2022

#### Keywords:

5G+  
Cascaded channel  
Channel estimation  
Convolutional neural networks  
FPGA

### ABSTRACT

Cascaded channels have been considered in several physical multipath propagation scenarios. However they are subject to phenomena such as multipath scattering, time dispersion and Doppler shift between the different links, which impose great challenges in relation to the channel estimation processing function in the receiver. In this paper we propose to tackle the problem of cascaded channels estimation in the fifth-generation and beyond (5G+) systems using convolutional neural networks (CNNs), without forward error correction (FEC) codes. The results show that the CNN-based framework reaches very close to perfect (theoretical) channel estimation levels, in terms of bit error rate (BER) values, and outperforms the least square (LS) practical estimation, measured in mean squared error (MSE). The benefits of CNN-based wireless cascaded channels estimation are particularly relevant for increasing number of links and modulation order. These findings are further confirmed at the CNN implementation stage on a field programmable gate array (FPGA) platform for a number of realistic quantization scenarios.

© 2022 Elsevier Inc. All rights reserved.

## 1. Introduction

In the literature, the wireless cascaded channel has gained attention, mainly due to its deployment in different communication scenarios [1–10]. Indeed, the wireless cascaded channel has been considered for cooperative vehicular [1], satellite [2] and multihop communications systems, relay stations [3–7], and in the context of intelligent reflecting surface (IRS) [8–10] for example.

Cascaded channels are subject to phenomena such as multipath scattering, time dispersion and Doppler shift between the different links, which impose great challenges in relation to the channel estimation processing function in the receiver. Thus, over the years, new estimation techniques have been proposed in order to deal with these issues and improve the global network performance, given the impact of the channel estimation processing function on it. In [3] for example, the performance analysis for multiple-relay amplify and-forward (AF) cooperative system over fading channels, with imperfect channel estimation, is presented. The authors in [3] demonstrate that a minimal imperfection in the channel es-

timation influences directly the overall performance of a system containing multiple-relay.

Regarding works that address practical and theoretical cascaded channel estimators, the authors in [4] use a predefined pilot matrix sequence in order to improve the channel estimation performance in a two-hop relay system using the least squares (LS) algorithm. In [5], a channel estimation process for dual hop multiple-input multiple-output (MIMO) orthogonal frequency division multiplexing (OFDM) relay networks is described, in which an iterative algorithm was enhanced in order to reduce the computational cost. Furthermore, in [6,7], new algorithms are proposed to decrease the channel estimation operation overhead in OFDM relay networks, due to the necessary number of  $N$  channel estimations.

Recently, encouraged by the significant advances of deep learning (DL), several studies have applied convolutional neural networks (CNNs) for wireless communication processing functions, including the channel estimation [11,12]. In this context, it is worth mentioning that DL is interesting given the ability to automatically extract the underlying representative characteristics of wireless communications. In addition, when compared with traditional methods for channel estimation, DL has the advantage of recognizing some patterns that mathematical algorithms cannot describe well, such as unknown and complex channel models, and non-linear problems.

\* Corresponding author.

E-mail address: fabiocoutinho@av.it.pt (F.D.L. Coutinho).

In 2004, the authors in [13] introduce machine learning (ML) for nonlinear channel estimation in MIMO systems, in which a new method for multiple variable regression estimation based on support vector machines (SVM) was developed. More recently, O’Shea and Hoydis [12] exposes the DL potential for the physical layer (PHY), highlighting the neural networks (NNs) ability to learn and compute the typical PHY processing functions. In [14], deep NNs were applied to the channel estimation and signal detection processing functions, in which a DL model was first trained offline to learn the channel distortion and interference statistics and then used for recovering the transmitted data. Furthermore, in [15], the power of CNNs to deal with the channel estimation function was demonstrated considering a fast fading communication channel. In [16], the authors describe the robustness of a CNN to the channel estimation for massive MIMO systems with pilot contamination. Kang, Chun and Kim shown in [17] that the CNNs are competent to perform the channel estimation function for MIMO systems with received signal-to-noise ratio (SNR) feedback in two fading scenarios, namely: quasi-static block and time-varying.

In addition, exploring the fifth-generation (5G) and beyond (5G+) trends, the results in [18] show that the deep CNNs are also effective in millimeter waves (mmWaves) massive MIMO systems. Also regarding 5G, it is investigated in [19,20] the influence of spatial correlation, Doppler shift and reference signal resource allocation in the channel estimation. The first one uses a two-dimensional (2D) CNNs architecture based on U-net, and a 3D CNNs architecture for handling spatial correlation. The last work uses a novel CNNs architecture to deal with various combinations of delay and doppler spread.

Motivated by the proven potential of the CNNs to perform channel estimation, in this paper we go further and study the benefits of CNN-based channel estimation processing function concerning particularly wireless cascaded channels in 5G+ systems, without forward error correction (FEC) codes. Each individual and independent link of the cascaded channel is characterized as a tapped delay line (TDL), typically the considered model in 5G networks. In addition, in contrast to the methodologies adopted in [5–7], in which the channel estimation is performed after each one of the links of the relay system, the proposed CNN estimator reduces these operations to only one in the receiver. That is, the algorithm proposed replaces the iterative process of conventional estimators and, consequently, reduces the overall complexity. In this study, the quality of the channel estimation processing function is evaluated by the mean squared error (MSE) metric and the overall performance of the system is assessed through the bit error rate (BER).

The major contributions of this work are summarized as follows:

- We propose to overcome the challenges in cascaded wireless channels estimation (multipath scattering, time dispersion and Doppler shift between the different links) by a CNN model. CNNs proved to be an advantageous channel gain estimator compared to the classical LS algorithm.
- We propose in this study to reduce the receiver complexity concerning the  $N$  wireless cascaded channel estimation processing functions. This complexity reduction is performed in the sense of the number of estimations, in which  $N$  estimators for each individual channel turn into one operation with CNNs, thus avoiding the iterations of conventional estimators, making it less expensive while maintaining a good performance.
- We adopted the TDL channel model, applied to 5G wireless communication scenarios, making this study an important contribution for several use cases related to 5G networks.
- We propose a CNN architecture optimized for wireless 5G cascaded channels, take into account a reasonable compromise

**Table 1**  
Features for 5G NR simulation.

5G NR features			
Bandwidth	100 MHz	Subcarriers	612
Numerology	1	Cyclic Prefix	Normal
Subcarrier Spacing	30 kHz	Number of Frames	600

between model accuracy, performance and training time. The aforementioned architecture is the result of a study in which several specifications were analyzed, including the validation frequency, the loss function, the maximum epochs, the shuffle operation, initial learn rate and the validation patience.

- The trained CNN is embedded on the field programmable gate array (FPGA) platform and tested in real time conditions with different fading channels. The FPGA prototype maintains close to perfect (theoretical) 5G+ channel estimation levels and outperforms the LS approach. Furthermore, a quantization study to evaluate the input data type impact on the CNNs performance in the FPGA was performed.

The remaining of this article is organized as follows. Section 2 describes the cascaded channel estimation approach using CNNs. In Section 3, the CNNs FPGA prototyping is explained. Results are shown in Section 4 and Section 5 is devoted to the conclusion.

## 2. CNN-based cascaded channel estimation

In this section, the approach concerning the cascaded channel estimation using CNNs is presented, in which the cascaded channel basic concepts, the end-to-end communication system, the CNNs architecture, and the global project flow are described.

### 2.1. End-to-end communication system

In this work, the 5G new radio (NR) communication system is considered, as defined by the 3rd generation partnership project (3GPP). Table 1 summarizes the adopted 5G features, which comply with 3GPP TR 38.211 Release 15 specifications for 5G NR standard [21]. The resource grid (RG) includes the physical downlink shared channel (PDSCH), the physical downlink shared channel-demodulation reference signal (PDSCH-DMRS) and the physical downlink shared channel-phase tracking reference signal (PDSCH-PTRS).

The end-to-end communication system implemented in this work is presented in Fig. 1. It consists of a typical 5G transmitter, a cascaded channel with  $N$  links and a 5G receiver. In the receiver, the CNN-based channel estimation is compared with both the perfect (theoretical) and the practical (LS) estimation approaches with respect to the MSE and the BER at the end of the 5G NR link. The necessary data for the overall CNN training, validation and test flow corresponds to the RG obtained after the OFDM demodulation and the perfect estimation complex values.

As observed in Fig. 1, the perfect timing and frequency synchronization is adopted so as not to interfere with the channel estimation results. In OFDM systems, which is the 5G NR case, timing and frequency offsets result in the rotation of the signal constellation, inter-symbol interference (ISI) and inter-carrier interference (ICI) [7], which can significantly deteriorate the system performance. Thus, as we aim to study the feasibility of the CNNs approach in the cascaded channel estimation, only the channel estimation processing function is analyzed considering the previous perfect synchronizations to prevent the propagation of errors. Likewise, FEC codes are not considered in the system model of this work due to the non-dependence of channel estimation with the related operation. FEC codes (i.e. low-density parity-check or

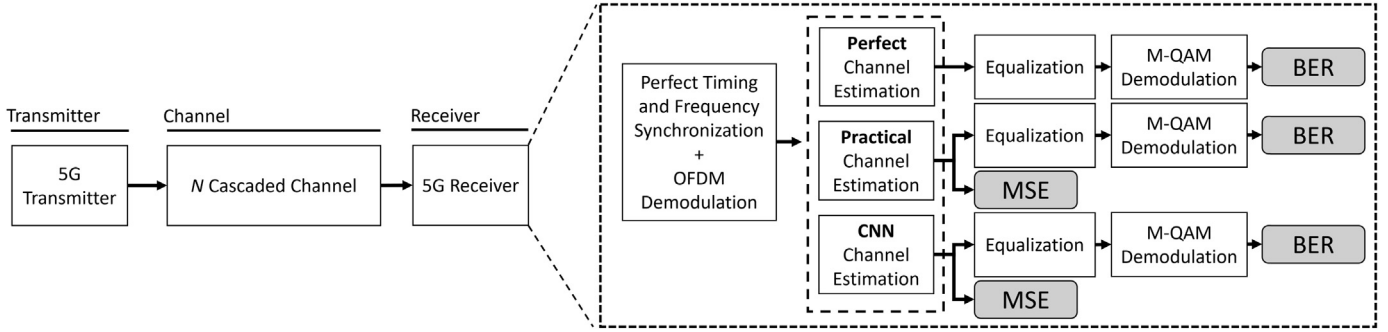


**Fig. 1.** Block diagram of the 5G NR end-to-end communication system.

**Table 2**  
TDL channel features for 5G NR simulation.

5G TDL channel features	
Delay Profile (DP)	TDL-A
Delay Spread (DS)	3e-7
Seed	0
Maximum Doppler Shift (MDS)	50

turbo codes) operate at the edge of the channel, where the transmitted data bits are encoded so that the received erroneous data bits can be recovered at the receiver. This means that the channel estimation is transparent to the aforementioned correction process.

Regarding the different approaches for the channel estimation, it should be mentioned that the perfect is obtained by the theoretical complex channel gains, being the reference values to the others. The practical channel estimation is provided by the interpolation of the channel response take into account the PDSCH-DMRS. Regarding the CNNs channel estimation, the received RG can be seen as a 2D image and thus, the channel estimation turns into an image processing problem. In fact, the CNNs are widely used in several computer vision tasks, such as image classification [22] and face recognition [23] for example. In Fig. 1, the 5G NR channel is characterized by the TDL, in which the fading model considered corresponds mainly to the Rayleigh and Rician, in some cases. In Table 2, the TDL channel features adopted in this work are presented. The number of multipaths, maximum Doppler shift, delay and power paths are standardized by European telecommunications standards institute (ETSI).

### 2.1.1. Cascaded channel system

As said in Section 1, cascaded channels have been considered in several physical multipath propagation scenarios. In this context, the block diagram of the TDL cascaded channels is presented in Fig. 2. In the aforementioned figure, the general system model corresponds to a set of time-independent channels in cascaded configuration, between the transmitter and receiver, represented in Fig. 1 as a box named *N Cascaded Channel*. Fig. 2 represents this cascaded channel model adopted in this work, in each TDL channel is represented by  $tdl_x$  and the additive white gaussian noise (AWGN) by  $n$ , in which  $x$  represents the number of the channel instantiation. Note that each channel corresponds to one independent channel generation.

### 2.2. CNN architecture

The present work was inspired by the results published in [16,18,19]. However, while in those studies CNNs are applied in one link channels, in this paper we extend the study to the far more challenging 5G (wireless) cascaded channel scenarios. Our model is a conventional CNN architecture (see Fig. 3), that con-

sists of an input layer with the size of  $612 \times 14$ , corresponding to the 5G features adopted in Table 1. The real and the imaginary part of each RG are subsequently input containing the interpolated PDSCH-DMRS symbols. Following the suggested CNN architecture in [16,18,19], three sets of convolutional and activation layers are used to extract and learn the representative characteristics (features) of the communication system. Finally, the output is a fully-connected regression layer, with the same dimension as the CNN input.

Description of the CNN layers is listed below.

- Input Layer: The interpolated PDSCH-DMRS is stored into a RG, and then separated into real and imaginary components. The CNN handles these components (real and imaginary) in a sequential mode (one after the other). Each 2D RG part is composed by 612 subcarriers per 14 symbols.
- Convolutional (Conv) Layers: The 2D RG data goes through a sequence of convolutional layers, composed by several filters, in order to extract channel features with different levels of complexity. The CNN architecture, shown in Fig. 3, was optimized to have 3 convolutional layers and convolution filters with  $9 \times 9$  and  $5 \times 5$  dimensions. In order to keep the original RG dimension (i.e.  $612 \times 14$ ), relevant paddings (Pad in Fig. 3) were added in the convolutional layers.
- Activation Layer: Rectified linear (ReLU) activation functions are applied over the feature maps produced by the convolutional layers.
- Output Regression Layer: Based on the features extracted from the hidden layers, the CNN outputs estimate the real and the imaginary part of the channel gain. Then, these parts are combined to get the complex channel gain.

The network optimal parameters (weights and biases) are obtained iteratively by minimizing the Loss function, defined as the half non-normalized MSE ( $MSE_{nn}$ ) for regression tasks. The Loss function between the estimated channel ( $\hat{y}_i$ ) and the actual channel ( $y_i$ ) is defined by

$$\text{Loss} = \frac{1}{2} \sum_{i=1}^n (\hat{y}_i - y_i)^2, \quad (1)$$

where  $n$  indicates the size of the training set. For better scaling and visualization, the evolution of the root-MSE (RMSE) during the training iterations was also monitored, and is given by

$$\text{RMSE} = \sqrt{\frac{1}{n} \sum_{i=1}^n (\hat{y}_i - y_i)^2}. \quad (2)$$

In Fig. 4, the RMSEs computed at each iteration with the training and the validation subsets respectively are presented. As can be

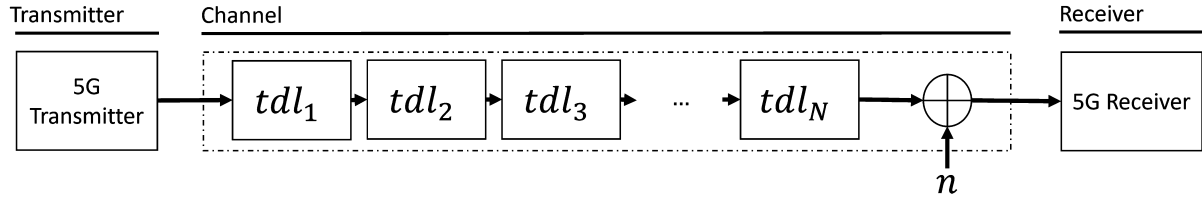


Fig. 2. Block diagram of the TDL cascaded channel model.

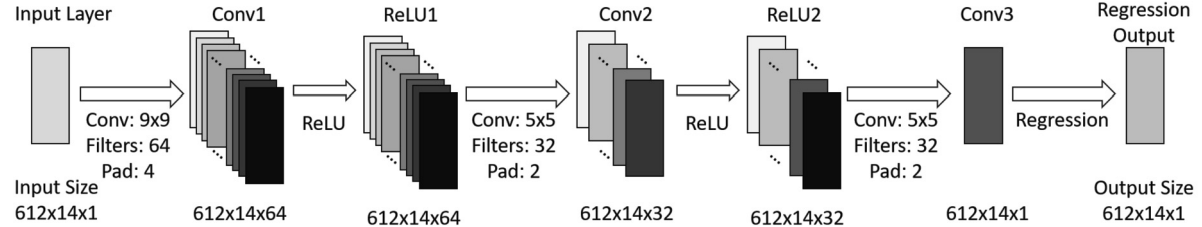


Fig. 3. CNNs structure for the channel estimation processing function.

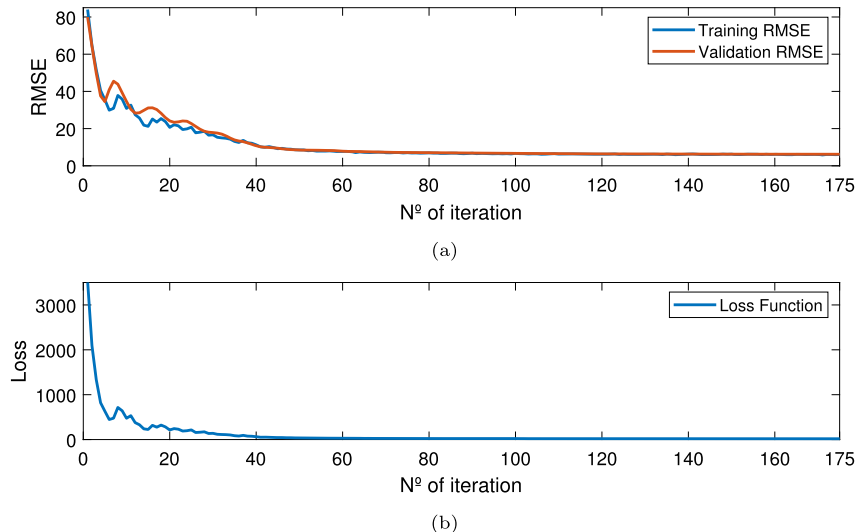


Fig. 4. RMSE obtained at each iteration during the training process.

seen the trajectories of both curves are close to each other which is an indication for the lack of overfitting issues. Similarly, regarding the Loss function, if the learning is successful, it is expected to converge to a constant and close to zero value, as it is shown in Fig. 4b.

The CNN training is related with the choice of a number of hyper-parameters. For the present model, the hyper-parameters that have significantly impact on the RMSE are the maximum epochs, the validation frequency, the validation patience, the initial learn rate, the optimization method (i.e. the optimizer) and data randomization (i.e. shuffling). All of them are related with the learning (optimization) process. The maximum epochs specifies the maximum number of training epochs. The validation frequency corresponds to how often (in terms of number of iterations) the validation RMSE is calculated. The validation patience is the number of epochs that the algorithm tries to improve the performance before giving up (if the error is not decreasing). The initial learn rate is a trade-off between training time (low initial learn rate) and overfitting (high initial learn rate). Two widely used optimization methods were compared, namely Adam and RMSprop. Finally, training with (at each epoch) or without data shuffling were also studied.

**Table 3**  
Set up of CNN hyper-parameters.

Hyper parameter	Range of values	Optimal value
Maximum Epochs	20, 25, 30, 35, 40, 45, 50, 55	45
Validation Frequency	1, 3, 5, 7, 9 times every epoch	5 times every epoch
Validation Patience	5, 10, 15, 20, 25, 30 epochs	15 epochs
Initial Learn Rate	3e-6, 3e-5, 3e-4, 3e-3, 3e-2	3e-4
Optimizer	Adam, RMSprop	Adam
Shuffle	Never, Every epoch	Every epoch

These parameters were optimized within a range of typical values, presented in Table 3, to achieve a reasonable compromise between model accuracy, performance and training time. The optimal values for the hyper parameters, are summarized in the third column of Table 3.

In Fig. 5 and Table 4 are presented the training and the validation RMSE, for the range of typical values of the hyper parameters. As optimal values were considered those that provided the lowest RMSE, or in alternative the minimum training time. Note that, as in Fig. 4, the training and the validation RMSEs for the chosen hyper parameters are close, which is again an indication for the lack of overfitting issues.

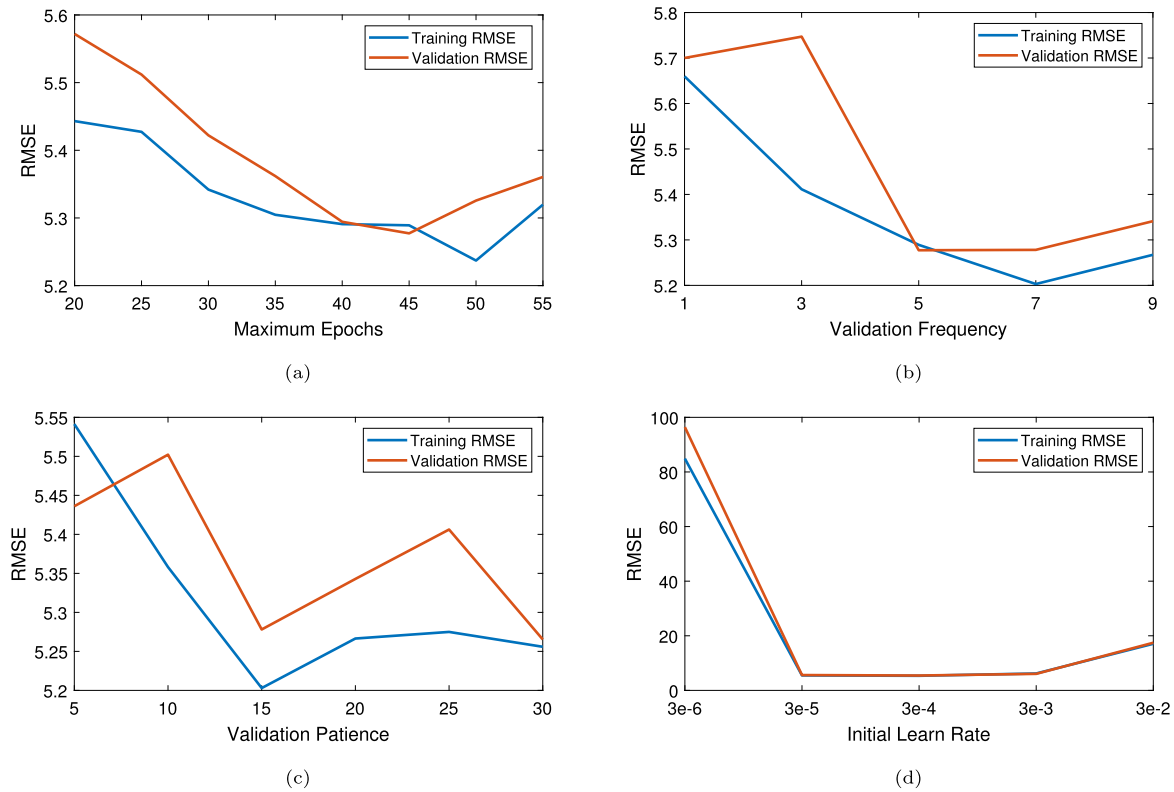


**Fig. 5.** RMSE for range of values of maximum epochs (a), validation frequency (b), validation patience (c), initial learn rate (d).

**Table 4**  
RMSE results for the optimizer and shuffle hyper parameters.

Hyper parameter	Optimizer		Shuffle	
	Adam	RMSprop	Never	Every epoch
Training RMSE	5.28	8.17	5.42	5.28
Validation RMSE	5.32	11.18	5.46	5.32

### 2.3. Training, validation and test flow

The overall flow performed in this study is schematically presented in Fig. 6. It consists of parameter configuration, training and validation steps, followed by model test and visualization of the results. Data was randomly generated and collected according to the 3GPP specifications with the system model shown in the Fig. 1, referred in Subsection 2.1. As said previously, the necessary data for the CNN training, validation and test flow corresponds to the RG obtained after the OFDM demodulation and the perfect estimation complex values. Thus, this data was randomly splitted into training (9600 RGs), validation (2400 RGs), and test (2400 RGs) sub-sets. The training and the validation steps are performed in-the-loop to control model overfitting problems. The simulation parameters were chosen such that each RG is subject to individual channel effects, covering a wide range of typical 5G channel effects. The final channel estimation quality was assessed by the MSE on test data (not used during the training and the validation steps). In addition, the overall channel performance, in terms of how well the transmitted bits are recovered, is evaluated by the test data BER.

### 3. CNN-based channel estimation on FPGA platform

The FPGA devices are widely used in wireless processing functions due to their real-time performance and the advantage of

being reconfigurable. As FPGAs are the major candidate for embedded devices in 5G networks, we tested the proposed channel estimation approach when the CNN-model is implemented on FPGA hardware.

In our analysis, a Zynq UltraScale+ MPSoC ZCU102 evaluation kit with a XCZU9EG-2FFVB1156 device is adopted in order to evaluate the trained CNNs. The overall flow considered in this work is shown in Fig. 7, in which the necessary configurations are previously performed, with CNN architecture loading, the FPGA selection, and the bitstream that contains the hardware configuration file. In detail, an ethernet connection is established from the computer to the FPGA, to load a firmware image in a secure digital (SD) card. This contains the support package with the embedded software and the FPGA programming file containing a generic DL processor intellectual property (IP) core. After that, the FPGA boot from the SD card is executed. Next, the compilation and the CNN deployment is done. For each loaded input data quantity, the estimation is delivered and the results are visualized, along with the latency report.

### 4. Results and discussion

In this section, we compare the BER and the MSE of the proposed CNN-based channel estimation with the perfect and the practical approaches for different SNR levels, number of links and modulation order. Perfect approach refers to the theoretical/ideal channel estimation and practical approach refers to the conventional LS method, a consolidated method for the channel estimation in cascaded channels [18]. The channel parameters are listed in Tables 1–2, and the CNN optimal hyper-parameters are listed in Table 3. The results here demonstrate the generalization properties of the CNN-based approach, because they are obtained with the test subset of the generated data, i.e. data not used to train or validate the CNN model.

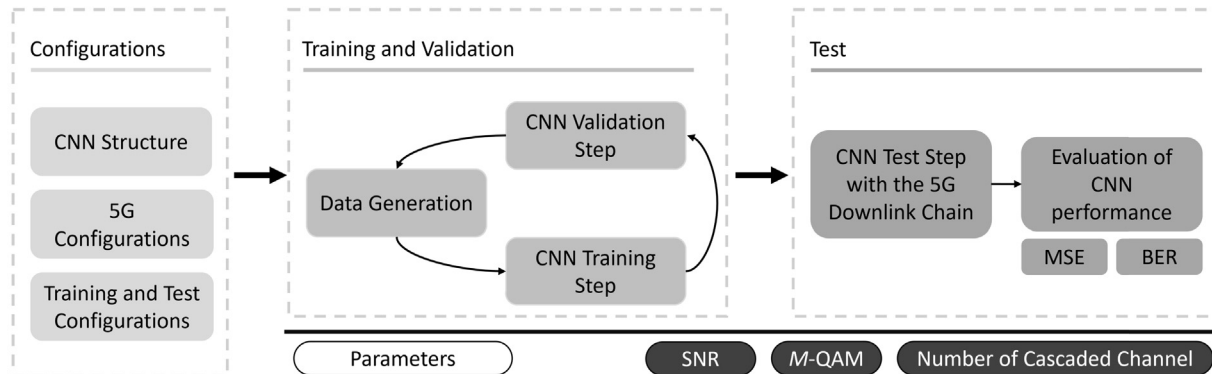


Fig. 6. CNN-based channel estimation flow diagram.

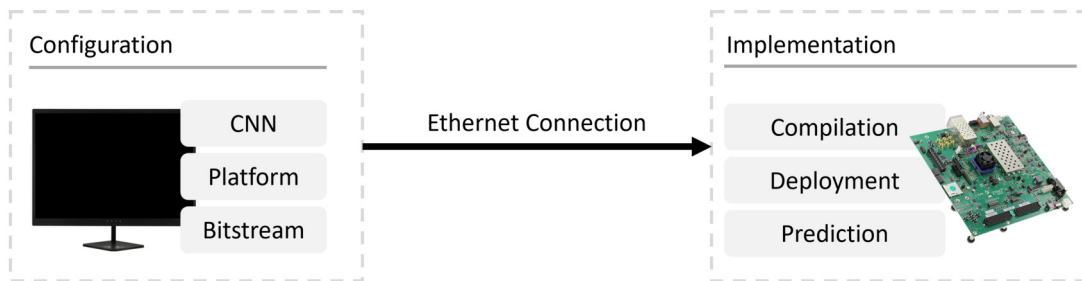
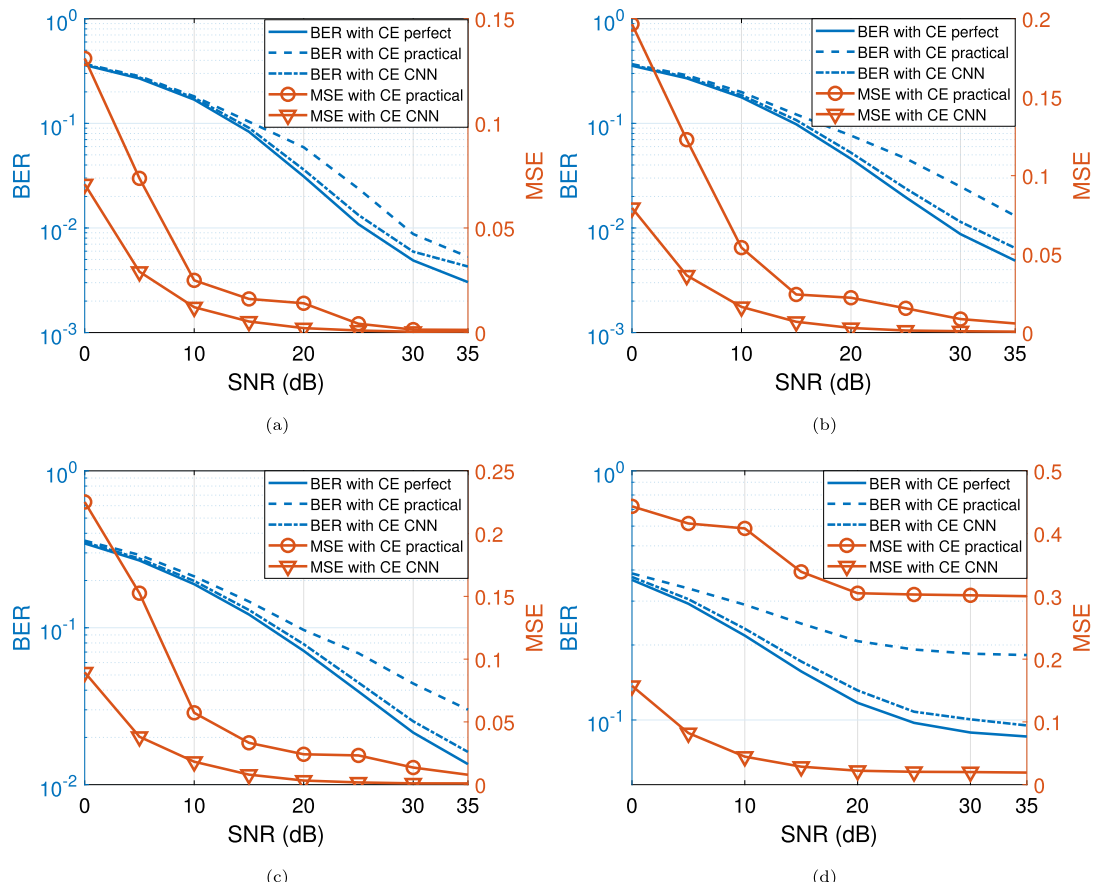
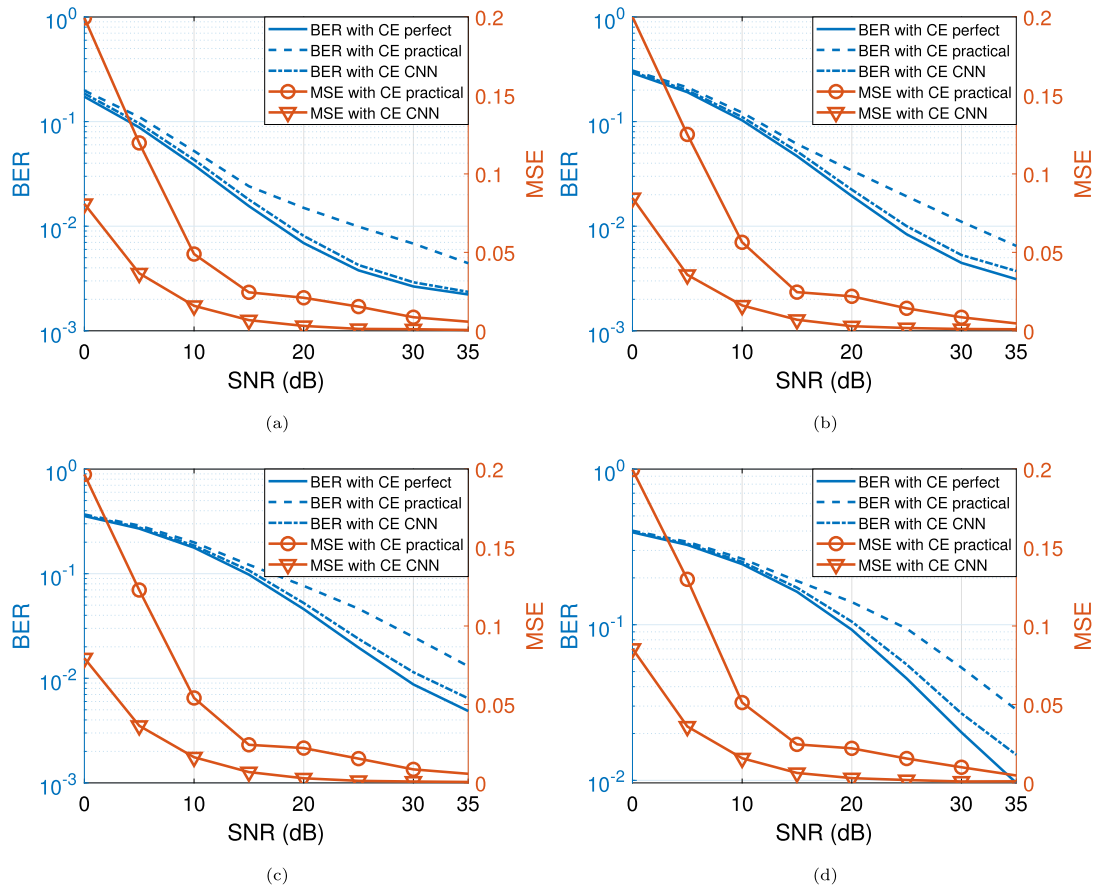


Fig. 7. FPGA prototyping flow to CNNs implementation on hardware.

Fig. 8. BER and MSE versus SNR, for constellation  $M = 64$  and varying number of links ( $N$ ): (a) 1 TDL channel, (b) 2 TDL channels, (c) 3 TDL channels and (d) 4 TDL channels. In the legend, CE is channel estimation.



**Fig. 9.** BER and MSE versus SNR, for  $N = 2$  channels and varying constellation (a)  $M = 4$ , (b)  $M = 16$ , (c)  $M = 64$  and (d)  $M = 256$ . In the legend, CE is channel estimation.

**Table 5**  
Nonidentical TDL channel features.

5G TDL channel features	Channel 1	Channel 2	Channel 3
Delay Profile (DP)	TDL-A	TDL-B	TDL-C
Delay Spread (DS)	3e-7	1e-7	0.3e-7
Seed	0	1	2
Maximum Doppler Shift (MDS)	50	100	25

In Fig. 8, BER and MSE curves are presented, for different number of cascaded channel links ( $N$ ), with the modulation order,  $M$ , of the  $M$ -ary quadrature amplitude modulation ( $M$ -QAM) scheme equal to 64 in 5G NR system. Initially, it should be mentioned that the BER measures presented in Fig. 8a are in accordance with [24], for the traditional techniques without FEC codes. In all cases (one, two, three or four TDL links) in Fig. 8 we observe that the CNN-based approach significantly reduces the MSE and outperforms the practical (LS) channel estimator. This is particularly notorious for low SNR levels (0–10 dB). For higher SNR (30–35 dB) both LS and CNN-based estimators tend to close MSE values. However, for the 4 links channel scenario (see Fig. 8d), even for high SNR levels the MSE of the practical estimator is much worse than the CNN-based counterpart. In terms of BER, while the CNN-based approach follows very closely the perfect estimator for the whole SNR range (0–35 dB), the practical approach worsens for higher SNR levels. Overall, the benefits of applying a deep learning approach are emphasized for increasing number of links. The negative effect of the increasing number ( $N$ ) of links in the cascaded channels, namely noise, fading, distortion, are significantly diminished when estimated by a data-based approach that certainly encodes better the channel specific characteristics than the practical (LS) approach.

In Fig. 9, BER and MSE versus SNR are shown considering the modulation order  $M$  equal to 4, 16, 64 and 256 symbols and cascaded channel with  $N = 2$  links. When  $M$  increases, the constellation symbols are closer and, consequently, they are more susceptible to the effects of the channel. This makes the receiver more likely to make mistakes in the decision process and therefore BER increases as seen in Fig. 9. However, the variation of  $M$  does not affect the channel estimation that much as the change of the channel links. Nevertheless, similar conclusions as in Fig. 8 can be drawn. The CNN-based channel estimator outperforms the practical approach in terms of smaller MSE for the lower SNR range (for all values of  $M$ ) and closer to the theoretical BER than the BER obtained with the practical estimator.

Simulated BER and MSE curves are shown in Fig. 10 as a function of the SNR, considering the channel estimation performed with the CNNs, perfect and practical approaches. In these simulations, nonidentical fading channels are adopted, since this is a more realistic scenario. The TDL channel features are described in Table 5. In addition, it is considered  $M = 256$  and  $N = 3$ . For comparison purposes, BER and MSE curves are also included in Fig. 10 taking into account the FPGA prototyping step. This study is performed in order to assess the CNN implementation feasibility for the 5G+ networks. In the FPGA experimental setup, there is an input data type quantization from 64 bits to 32 bits in floating point, resulting in a relative error mean between the two implementations in the order of  $10^{-8}$ , concerning of MSE, with the BER unchanged, thus justifying the applicability and implementation of CNNs in FPGAs in several practical scenarios, which made this framework rather plausible. Thus, if an architecture with 32 bits in floating point is considered, it should be mentioned that the error obtained is basically due to the truncation of the number of bits.

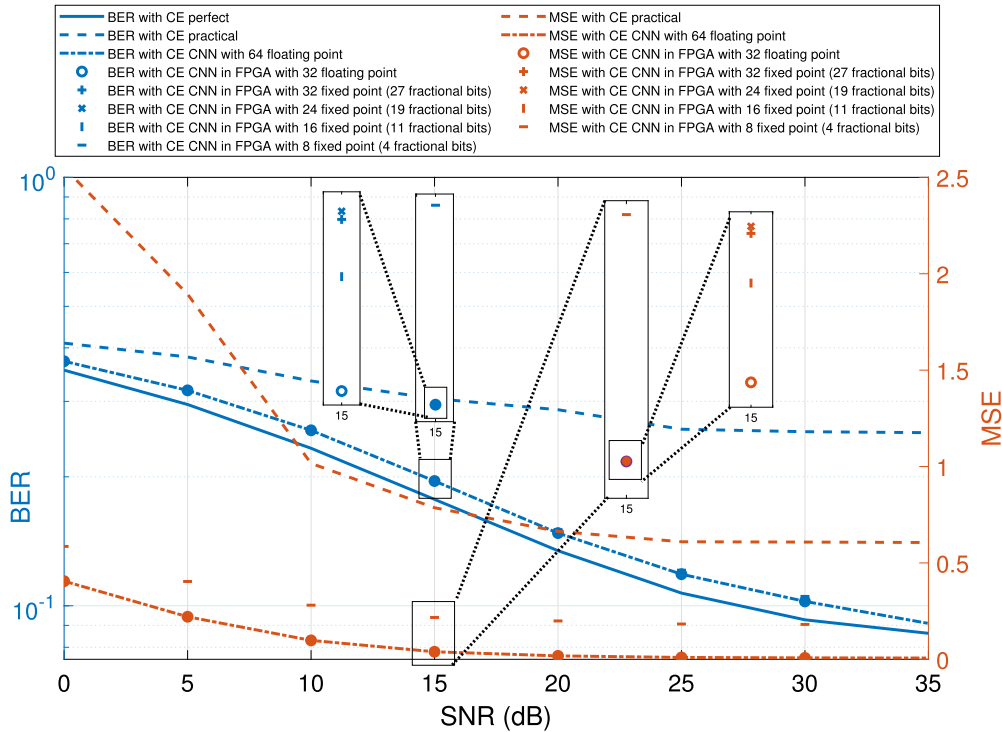


**Fig. 10.** BER and MSE versus SNR. Comparison between CNN-based cascaded channel estimator in FPGA hardware, Perfect and Practical (LS) approaches. 3 nonidentical fading channels and  $M = 256$  are adopted. In the legend, CE is channel estimation.

In our work, the impact of the number of input data bits in a more realistic implementation, that is, with a smaller number of bits combined with a fixed point architecture, is also analyzed in order to maximize the overall performance of the wireless network. For this input data type quantization study, a set of four fixed point configurations is also included in Fig. 10 in order to compare the BER and MSE values between them, namely: 32 bits with 27 fractional places, 24 bits with 19 fractional places, 16 bits with 11 fractional places, and 8 bits with 4 fractional places. The choice of the length regarding the integer and fractional bits results in a careful study in which the relative error between the implementations is minimized. From the results presented in Fig. 10, it is possible to verify that the BER and MSE curves concerning the CNNs implementation in software and in FPGA have an excellent match. The difference in the channel estimation in terms of the MSE metric, looking to the relative error mean (quantization error), is shown in Table 6 taking the 32 bits in floating point implementation as reference. The results obtained are directly affected by the bit length, in which the behavior of the quantization error follows the decrease in the number of bits. The impact of this quantization study on BER is also dependent on the number of bits, as shown in Table 6. However, the impact is smaller in the order of two decimal places than in the MSE metric. Regarding the FPGA implementation feasibility study, it is important to consider the input data type impact in the global performance system. For example, from the case with 32 bits (floating point) to the 8 bits (fixed point), the quantization error is  $10^{-4}$ , which imposes a BER increasing in the order of the  $10^{-2}$ . This means that the data input type quantization step has a considerable impact on the overall system and it is necessary to take it into account in the real system implementation.

In terms of CNNs latency, Table 7 shows the obtained performance during the FPGA implementation step considering the clock frequency equal to 220 MHz. Note that the layers that introduce more latency are the convolutionals, since the activation ones corresponds only to a function executed in a clock cycle. This result

**Table 6**  
Quantization errors regarding MSE and BER metrics.

Input data type	MSE quantization error	BER quantization error
32 (24 fractional) bits	$10^{-7}$	$10^{-5}$
24 (19 fractional) bits	$10^{-6}$	$10^{-4}$
16 (11 fractional) bits	$10^{-5}$	$10^{-3}$
8 (4 fractional) bits	$10^{-4}$	$10^{-2}$

**Table 7**  
CNN latency due to FPGA implementation, for clock frequency = 220 MHz.

CNNs implementation latency		
Layer	Clock cycles	Seconds
Conv1	1558743	0.00709
Conv2	5066715	0.02303
Conv3	546545	0.00248
All Layers	7171961	0.03260

proves the CNN implementation feasibility in the FPGA platform, relatively to the necessary processing time.

## 5. Conclusions

In this paper, cascaded channel estimation in the fifth-generation and beyond (5G+) systems using convolution neural network (CNN), without forward error correction (FEC) codes, was proposed. In addition, the CNN prototyping was also performed, employing the field programmable gate array (FPGA) platform. The results of the implementation of CNNs on FPGA hardware in several realistic scenarios, revealed this deep data-based framework as very promising. Furthermore, the impact of the number of bits combined with a fixed point architecture was also analyzed. The results of the quantization study have shown that the performance of the 5G and 5G+ wireless networks can be significantly enhanced by a CNN-based channel estimation embedded in FPGA hardware.

In addition, the  $N$  estimators for each individual channel was turned into one operation with CNNs, thus avoiding the iterations of conventional estimators and reducing the receiver complexity. Several experimental and simulation results were obtained, concerning mean squared error (MSE) and bit error rate (BER) under different number of links and modulation order. These results show that the CNN-based framework reaches very close to perfect (theoretical) channel estimation levels, in terms of BER values, and outperforms the LS practical estimation, measured in MSE. This indicates that the proposed CNN-based channel estimator has the potential to mitigate the negative effects of channels with several links and recover reliably the real and imaginary parts of the channel complex gains. In all studied scenarios, the CNN-based wireless cascaded channel estimator outperformed the conventional LS technique. These findings are particularly relevant for increasing number of links and increasing modulations orders.

As future work, a system model with real synchronization processes will be considered, in which the symbol timing detection and carrier frequency offset algorithms are taken into account in order to verify the impact on the CNN-based channel estimation processing function. It should be mentioned that this case is considered more appropriate and of practical interest to characterize more realistic 5G scenarios, since the timing and frequency offsets caused by absent of perfect synchronization result in the rotation of the signal constellation, imposed by the inter-symbol interference and inter-carrier interference, which can significantly deteriorate the system performance. Furthermore, an exhaustive study with different 5G new radio configurations can be performed.

### CRediT authorship contribution statement

Fábio D. L. Coutinho and Hugerles S. Silva carried out the simulations. Petia Georgieva and Arnaldo S. R. Oliveira performed the technical review and analysis of the results. Fábio D. L. Coutinho, Hugerles Silva, Petia Georgieva and Arnaldo S. R. Oliveira wrote the paper. All authors read and approved the final manuscript.

### Declaration of competing interest

The authors declare that they have no known competing financial interests or personal relationships that could have appeared to influence the work reported in this paper.

### Acknowledgments

This work was supported by FCT/MCTES through national funds and, when applicable, co-funded by EU funds under the project UIDB/50008/2020-UIDP/50008/2020. It was also developed in the scope of the Project Augmented Humanity [POCI-01-0247-FEDER-046103 and LISBOA-01-0247-FEDER-046103], financed by Portugal 2020, under the Competitiveness and Internationalization Operational Program, the Lisbon Regional Operational Program, and by the European Regional Development Fund.

### References

- [1] H. İlhan, Performance analysis of cooperative vehicular systems with co-channel interference over cascaded Nakagami- $m$  fading channels, *Wirel. Pers. Commun.* 83 (Feb. 2015) 203–214.
- [2] M.K. Arti, Channel estimation and detection in satellite communication systems, *IEEE Trans. Veh. Technol.* 65 (12) (Dec. 2016) 10173–10179.
- [3] Y.M. Khattabi, M.M. Matalgah, Performance analysis of multiple-relay AF cooperative systems over Rayleigh time-selective fading channels with imperfect channel estimation, *IEEE Trans. Veh. Technol.* 65 (1) (Jan. 2016) 427–434.
- [4] J. Ma, P. Orlik, J. Zhang, G.Y. Li, Pilot, Matrix design for estimating cascaded channels in two-hop MIMO amplify-and-forward relay systems, *IEEE Trans. Wirel. Commun.* 10 (6) (Jun. 2011) 1956–1965.

- [5] A.P. Millar, S. Weiss, R.W. Stewart, Training-based channel estimation algorithms for dual hop MIMO OFDM relay systems, *IEEE Trans. Commun.* 63 (12) (Dec. 2015) 4711–4726.
- [6] F. Tseng, W. Huang, W. Wu, Robust far-end channel estimation in three-node amplify-and-forward MIMO relay systems, *IEEE Trans. Veh. Technol.* 62 (8) (Oct. 2013) 3752–3766.
- [7] R. Wang, H. Mehrpouyan, M. Tao, Y. Hua, Channel estimation, carrier recovery, and data detection in the presence of phase noise in OFDM relay systems, *IEEE Trans. Wirel. Commun.* 15 (2) (Feb. 2016) 1186–1205.
- [8] Y. Liu, S. Zhang, F. Gao, J. Tang, O.A. Dobre, Cascaded channel estimation for RIS assisted mmWave MIMO transmissions, *IEEE Wirel. Commun. Lett.* 10 (9) (Sept. 2021) 2065–2069.
- [9] C. You, B. Zheng, R. Zhang, Wireless communication via double IRS: channel estimation and passive beamforming designs, *IEEE Wirel. Commun. Lett.* 10 (2) (Feb. 2021) 431–435.
- [10] H. Liu, X. Yuan, Y.-J.A. Zhang, Matrix-calibration-based cascaded channel estimation for reconfigurable intelligent surface assisted multiuser MIMO, *IEEE J. Sel. Areas Commun.* 38 (11) (Nov. 2020) 2621–2636.
- [11] T. Wang, C.K. Wen, H. Wang, F. Gao, T. Jiang, S. Jin, Deep learning for wireless physical layer: opportunities and challenges, *China Commun.* 14 (11) (Oct. 2017) 92–111.
- [12] T. O'Shea, J. Hoydis, An introduction to deep learning for the physical layer, *IEEE Trans. Cogn. Commun. Netw.* 3 (4) (Dec. 2017) 563–575.
- [13] M. Sanchez-Fernandez, M. de-Prado-Cumplido, J. Arenas-Garcia, F. Perez-Cruz, SVM multiregression for nonlinear channel estimation in multiple-input multiple-output systems, *IEEE Trans. Signal Process.* 52 (8) (Aug. 2004) 2298–2307.
- [14] H. Ye, G.Y. Li, B. Jiang, Power of deep learning for channel estimation and signal detection in OFDM systems, *IEEE Wirel. Commun. Lett.* 7 (1) (Feb. 2018) 114–117.
- [15] M. Soltani, V. Pourahmadi, A. Mirzaei, H. Sheikhzadeh, Deep learning-based channel estimation, *IEEE Commun. Lett.* 23 (4) (Apr. 2019) 652–655.
- [16] H. Hirose, T. Ohtsuki, G. Gui, Deep learning-based channel estimation for massive MIMO systems with pilot contamination, *IEEE Open J. Veh. Technol.* 2 (Dec. 2020) 67–77.
- [17] J. Kang, C. Chun, I. Kim, Deep learning based channel estimation for MIMO systems with received SNR feedback, *IEEE Access* 8 (Jul. 2020) 121162–121181.
- [18] P. Dong, H. Zhang, G.Y. Li, I.S. Gaspar, N. NaderiAlizadeh, Deep CNN-based channel estimation for mmWave massive MIMO systems, *IEEE J. Sel. Top. Signal Process.* 13 (5) (Sep. 2019) 989–1000.
- [19] B. Marinberg, A. Cohen, E. Ben-Dror, H.H. Permuter, A study on MIMO channel estimation by 2D and 3D convolutional neural networks, in: Proceedings of the IEEE International Conference on Advanced Networks and Telecommunications Systems, 2020, pp. 1–6.
- [20] P. Saikrishna, A.K.R. Chavva, M. Beniwal, A. Goyal, Deep learning based channel estimation with flexible delay and Doppler networks for 5G NR, in: Proceedings of the IEEE Wireless Communications and Networking Conference, 2021, pp. 1–6.
- [21] 3GPP. Physical Channels and Modulation. In Specification of the 3rd Generation Partnership Project (3GPP), Tech. Report 38.211, ver. 16 Jun. 2018.
- [22] A. Krizhevsky, I. Sutskever, G.E. Hinton, ImageNet classification with deep convolutional neural networks, *Adv. Neural Inf. Process. Syst.* 25 (Dec. 2012) 1097–1105.
- [23] Y. Sun, Y. Chen, X. Wang, X. Tang, Deep learning face representation by joint identification-verification, *Adv. Neural Inf. Process. Syst.* 2 (Jun. 2014) 1988–1996.
- [24] S.H. Myint, K. Yu, T. Sato, Modeling and analysis of error process in 5G wireless communication using two-state Markov chain, *IEEE Access* 7 (Jan. 2019) 26391–26401.



**Fábio D. L. Coutinho** received the B.Sc. and M.Sc. degrees on Electronics and Telecommunications from University of Aveiro, Portugal, in 2019. He is currently pursuing the Ph.D. degree in Electrical Engineering from the same university. He is currently a researcher at Telecommunications Institute - Aveiro. His current research interests include the next generation radio access networks, reconfigurable digital systems, physical layer and machine learning.



**Hugerles S. Silva** received his B.Sc., M.Sc. and Ph.D. degrees in Electrical Engineering from University Federal of Campina Grande, Brazil, in 2014, 2016 and 2019, respectively. He is currently an adjunct professor at the University of Brasília. His main research interests include wireless communication, digital signal processing and wireless channel modeling.



communications.

**Petia Georgieva** is Professor of Machine Learning in the Department of Electronics Telecommunications and Informatics (DETI) at University of Aveiro, Portugal and senior researcher in the Institute of Electronics Engineering and Telematics of Aveiro (IEETA), Portugal. Her research interests include machine learning, deep learning and data mining with strong application focus on brain computer interface, medical imaging, robotics, and more recently optical and wireless



**Arnaldo S. R. Oliveira** received the Ph.D. degree on Electrical Engineering in 2007 from the University of Aveiro, Portugal. He also holds the B.Sc. and M.Sc. degrees, both on Electronics and Telecommunications, from the same university. He is currently a researcher at Telecommunications Institute – Aveiro and since 2001 he teaches computer architecture, digital systems design, programming languages and embedded systems at the University of Aveiro, where he is now an Assistant Professor. His research interests include reconfigurable digital systems, software defined radio and next generation radio access networks. He participates in several national and European funded research projects. He is the author or co-author of more than 100 journal and international conference papers.